

Deterministic amplification of Schrödinger cat states in circuit quantum electrodynamics

Jaewoo Joo,^{1,2} Matthew Elliott,² Daniel K. L. Oi,³ Eran Ginossar,² and Timothy P. Spiller⁴

¹*Quantum Information Science, School of Physics and Astronomy, University of Leeds, Leeds LS2 9JT, U.K.*

²*Advanced Technology Institute and Department of Physics,
University of Surrey, Guildford, GU2 7XH, United Kingdom*

³*SUPA Department of Physics, University of Strathclyde, Glasgow, G4 0NG, United Kingdom*

⁴*York Centre for Quantum Technologies, Department of Physics, University of York, York YO10 5DD, U.K.*

(Dated: August 6, 2022)

We propose a dynamical scheme for deterministically amplifying photonic Schrödinger cat states based on a set of optimal state-transfers. The scheme can be implemented in strongly coupled qubit-cavity systems and is well suited to the capabilities of state of the art superconducting circuits. The ideal analytical scheme is compared with a full simulation of the open Jaynes-Cummings model with realistic device parameters. This amplification tool can be utilized for practical quantum information processing in non-classical continuous-variable states.

PACS numbers: 42.65.Yj, 42.50.Pq, 85.25.Hv, 03.65.Yz

Superpositions of two large coherent states with opposite phases, called Schrödinger cat states (SCSs) [1], are a canonical example of macroscopic superposed states and have great potential to open up new avenues for quantum technology, including continuous-variable (CV) quantum communication [2], quantum computation [3–5], teleportation [6], and quantum metrology [7, 8]). Fault-tolerant CV quantum computing can be achieved using only linear optics if the size of the SCSs is appropriate to keep the orthogonality of coherent states as well as to prevent excessive decoherence [3–5]. These applications provide significant motivation to engineer SCS amplification.

Realisation of a large enough amplitude SCSs is non-trivial in general, and perfect amplification of SCSs of unknown size is not possible because amplification of coherent states (i.e., $|\alpha\rangle \rightarrow |G\alpha\rangle$ for $G > 1$), which could also amplify SCSs, introduces unavoidable excess noise [9]. However, probabilistic linear amplification of a coherent state with high fidelity is feasible by adding and subtracting single photons [10, 11]. Note that optical amplification operators, for example $\hat{a}\hat{a}^\dagger$ and $(\hat{a}^\dagger)^2$, behave differently to the one proposed here with respect to input α and amplification rate G [12, 13] and a two-photon loss environment could be beneficial to create/stabilize the SCSs [14, 15]. An amplification scheme with two known amplitude SCSs [16, 17] and probabilistic methods of amplifying SCSs have recently been developed in quantum optics [6, 18].

The rapid development of circuit-quantum electrodynamics (QED) technology could provide a new platform for scalable quantum systems. The Josephson non-linearity allows the production of superconducting artificial atoms which can be coupled to a 3D cavity containing microwave photons. Sufficiently large SCSs ($\alpha \approx 2$) [14, 19] and generalized Fock states [20] have very recently been generated in a cavity field with the assistance of a superconducting qubit. The enhanced stabilization

of SCSs in a cavity has been recently reported in a specially designed lossy environment [14, 21] and this architecture could be useful for robust quantum memory [22]. Thus, amplification of SCSs would benefit a wide range of CV quantum technologies, particularly a new type of quantum computation in circuit-QED [23].

In this Letter, we propose a deterministic scheme for amplifying an SCS in superconducting circuits. The key difference between optics-only and atom-assisted methods is that the amplification can be performed deterministically. Our scheme is inspired by the fact that applying the two-photon shift operation [24], $(\hat{E}^\dagger)^2 : |m\rangle \rightarrow |m+2\rangle$, one or more times on even/odd SCSs preserves their even/odd distribution of amplitudes while $(\hat{a}^\dagger)^2 : |m\rangle \rightarrow \sqrt{(m+2)!/m!} |m+2\rangle$ with a renormalization. We analyze and simulate the operation \hat{E}^\dagger on a SCS in a cavity coupled to a transmon qubit in the presence of decoherence [25]. For this scheme, we find fast controls, which perform all the state-transfers required for \hat{E}^\dagger operation on SCS with high fidelity well within realistic decoherence time ($\approx 6\mu s$) in circuit-QED.

We generalize the notion of amplification to the case where an initial SCS $|SC_\alpha^\pm\rangle$ is transformed by an operation \hat{A} into a state $\hat{A}|SC_\alpha^\pm\rangle$ that approximates a coherent state superposition $|SC_{\alpha'}^\pm\rangle$ where $\alpha' > \alpha$,

$$|SC_{\alpha'}^\pm\rangle \approx \hat{A}|SC_\alpha^\pm\rangle = \sum_{k=0}^{\infty} c_k |k+b\rangle \langle k| SC_\alpha^\pm, \quad (1)$$

where an even/odd Schrödinger cat state is given by

$$|SC_\alpha^\pm\rangle = \mathcal{N}_\alpha^\pm (|\alpha\rangle \pm |-\alpha\rangle), \quad (2)$$

for some normalisation \mathcal{N}_α^\pm ($b > 0$). Due to destructive interference between $|\alpha\rangle$ and $|-\alpha\rangle$, even SCSs only have even photon numbers while odd SCSs only have odd photon numbers. Note that c_k is determined by the am-

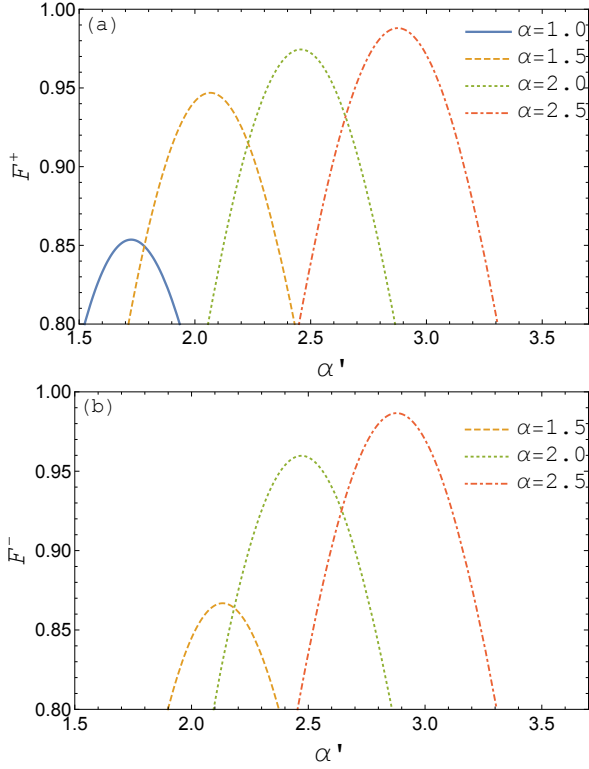


FIG. 1. Fidelities \mathcal{F}^\pm between $(\hat{E}^\dagger)^2 |SC_\alpha^\pm\rangle$ and amplified state $|SC_{G\alpha}^\pm\rangle$ for starting amplitudes $\alpha = 1.0, 1.5, 2.0, 2.5$. (a) \mathcal{F}_{max}^+ are 0.854, 0.947, 0.974, 0.988 with $G \approx 1.725, 1.377, 1.229, 1.151$. (b) \mathcal{F}_{max}^- are 0.681, 0.866, 0.960, 0.987 with $G \approx 1.902, 1.422, 1.235, 1.151$.

plification operator \hat{A} .

If we apply the two photon shift operator l times, $\hat{A} = (\hat{E}^\dagger)^{2l}$, where

$$(\hat{E}^\dagger)^{2l} = \sum_{m=0}^{\infty} |m+2l\rangle \langle m|, \quad (3)$$

normalisation is preserved and the operation simply shifts the Fock state amplitude distribution. It can therefore be performed deterministically in principle [31], producing an approximation of an amplified SCS $|SC_{\alpha'}^\pm\rangle$. Fig. 1 shows the results of applying $(\hat{E}^\dagger)^2$ to both even and odd SCSs and calculating the overlap of an amplified SCS $(\hat{E}^\dagger)^2 |SC_\alpha^\pm\rangle$ with an expected SCS $|SC_{\alpha'}^\pm\rangle$, where the fidelities are

$$\mathcal{F}^\pm = \left| \langle SC_{\alpha'}^\pm | (\hat{E}^\dagger)^2 | SC_\alpha^\pm \rangle \right|^2. \quad (4)$$

We quantify the amplification by the value G , defined by $\alpha' = G\alpha$ which maximises \mathcal{F}^\pm , giving the closest SCS to $(\hat{E}^\dagger)^2 |SC_\alpha^\pm\rangle$,

$$G = \arg \max_{G'} \left| \langle SC_{G'\alpha}^\pm | (\hat{E}^\dagger)^2 | SC_\alpha^\pm \rangle \right|^2 \quad (5)$$

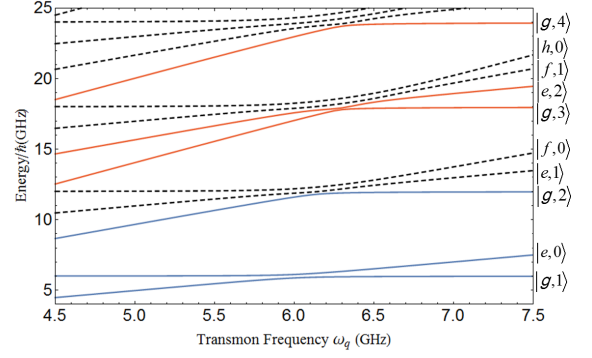


FIG. 2. Energy level structure of transmon coupled to a cavity with $\omega_r = 6\text{GHz}$ and $\lambda = 0.1\text{GHz}$ [34]. Solid lines indicates a set of Λ -type levels $\{|+, n\rangle, |-, n\rangle, |-, n+1\rangle\}$ suitable for state-transfers and dashed lines are other eigenstates of the Hamiltonian in Eq. (6) [25, 26]. The labels on the right hand side are the product states that approximate the eigenstates for large positive detunings $((\omega_q - \omega_r)/\lambda \gg 1)$.

In general, the maximum fidelity \mathcal{F}_{max}^\pm approaches 1 for large α but G also tends to 1, indicating no amplification at very large SCSs using $(\hat{E}^\dagger)^2$, but stabilisation on the input SCS persists. Interestingly, for small α , $(\hat{E}^\dagger)^2$ works better for even SCSs because $|SC_\alpha^- \rangle$ for $\alpha \approx 0$ becomes a one-photon Fock state. This amplified small $|SC_\alpha^- \rangle$ maps to a three-photon Fock state, which is very different to any odd SCS (e.g. $\mathcal{F}_{max}^- < 0.8$ for $\alpha = 1.0$ in the bottom figure of Fig. 1). This feature disappears for $\alpha \approx 1.5$ because $|\alpha\rangle$ is sufficiently orthogonal to $|- \alpha\rangle$.

Implementation of \hat{E}^\dagger in circuit-QED – Here we demonstrate a scheme for deterministically performing \hat{E}^\dagger on a cavity field with the assistance of an artificial atom. Due to large nonlinearity, circuit-QED provides a suitable parameter range for amplification of SCSs, and we show a state-transfer scheme adapted from the original idea of stimulated Raman adiabatic passage (STIRAP) in a cavity-QED setup [27–30]. One important advantages of this scheme is that \hat{E}^\dagger is deterministic while \hat{E} is probabilistic, which has been proposed to experimentally measure expectation values of \hat{E} , \hat{E}^\dagger and $\hat{E}^\dagger \hat{E} = \mathbb{1} - |0\rangle\langle 0|$ [30, 31]. Conventional STIRAP has also been demonstrated in circuit-QED [32, 33].

Our amplification operation can be realised with a set of STIRAP-inspired pulses implemented within the qubit-cavity level structure in conjunction with dynamical control via varying local fluxes [34, 35]. In contrast to the conventional cavity-QED setup with a bare atomic Λ -level configuration, we use a set of Λ -type systems in the dressed Jaynes-Cummings (JC) model where the cavity and qubit are on resonance [25]. The key operation is efficient state-transfer from $|+, n\rangle$ to $|-, n\rangle$. This is compatible with the architecture for creating SCSs in [19].

We model a transmon coupled to a cavity by a gener-

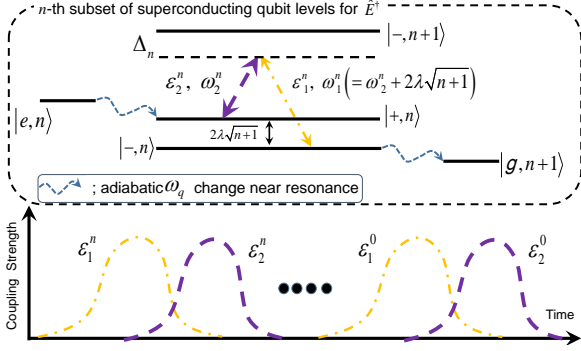


FIG. 3. STIRAP-inspired pulse sequence to realise \hat{E}^\dagger . (Top) An adiabatic sweep of the qubit frequency ω_q into resonance with the cavity ω_r transforms an initial state $|e, n\rangle$ into the dressed state $|+, n\rangle$. Next a microwave field is first applied between $|-, n\rangle$ and $|-, n+1\rangle$ with time dependent amplitude $\epsilon_1^n(t) = |\epsilon_1^n| \exp[-(t-\tau)^2/T^2]$ and frequency ω_1^n (yellow dot-dashed line), followed by another field driving the second transition ($|+, n\rangle \leftrightarrow |-, n+1\rangle$) ($\epsilon_2^n(t) = |\epsilon_2^n| \exp[-(t+\tau)^2/T^2]$, ω_2^n in purple dashed). For a SCS, the $|-, n+1\rangle$ state is unpopulated hence does not participate in the dynamics. There is non-zero overlap between the pulses determined by the temporal offset τ . The microwave frequencies are detuned Δ_n from the $|-, n+1\rangle$ state but satisfy the two-photon transition condition, $\omega_1^n - \omega_2^n = 2\lambda\sqrt{n+1}$. For efficient transfer of $|+, n\rangle \rightarrow |-, n+1\rangle$, we require $\tau > (\sqrt{2}-1)T$ and $|\epsilon|T \gg 10$ [32]. After the counterintuitive pulse sequence, a further adiabatic sweep of the transmon frequency back up out of resonance results in $|g, n+1\rangle$, disentangling the atom from the cavity which is now in the state $\sum c_n |n+1\rangle = \hat{E}^\dagger \sum c_n |n\rangle$.

alised JC Hamiltonian

$$\hat{H}^t = \omega_r \hat{a}^\dagger \hat{a} + \sum_j \frac{\omega_{qj}}{2} |j\rangle\langle j| + \sum_{j,k} \lambda_{j,k} (\hat{a}^\dagger |j\rangle\langle k| + \hat{a} |k\rangle\langle j|), \quad (6)$$

for transmon energy levels $j, k = \{g, e, f, h, \dots\}$ and transmon-cavity couplings $\lambda_{j,k}$. As shown in Fig. 2, when the transmon frequencies are far from resonance with the cavity, the bare states are given by $|j, n\rangle$ with transmon state j and photon number n , while they become dressed states at near resonance. Considering only two transmon levels, $\{|g\rangle, |e\rangle\}$, the eigenstates are

$$|+, n\rangle = \cos \theta_n |e, n\rangle + \sin \theta_n |g, n+1\rangle, \quad (7)$$

$$|-, n\rangle = -\sin \theta_n |e, n\rangle + \cos \theta_n |g, n+1\rangle, \quad (8)$$

where $\omega_q = \omega_{qg}$ is the $|g\rangle \leftrightarrow |e\rangle$ transition frequency, $\lambda = \lambda_{g,e}$ is the qubit-cavity coupling, and $2\theta_n = \tan^{-1}(2\lambda\sqrt{n+1}/\delta)$, with $\delta = \omega_q - \omega_r$. Note that $|+, n\rangle \approx |e, n\rangle$ and $|-, n\rangle \approx |g, n+1\rangle$ for large δ , so if we start in $|e, n\rangle$ far from resonance, the state adiabatically becomes $|+, n\rangle$ near resonance $\delta \approx 0$.

The protocol for performing \hat{E}^\dagger , illustrated in Fig. 3, is as follows. (1) An SCS $|SC_\alpha^\pm\rangle_c = \sum_{n=0}^\infty c_n |n\rangle_c$ is initially prepared in the cavity, with the qubit in $|e\rangle_q$ and far detuned from the cavity frequency ω_r . (2) We adi-

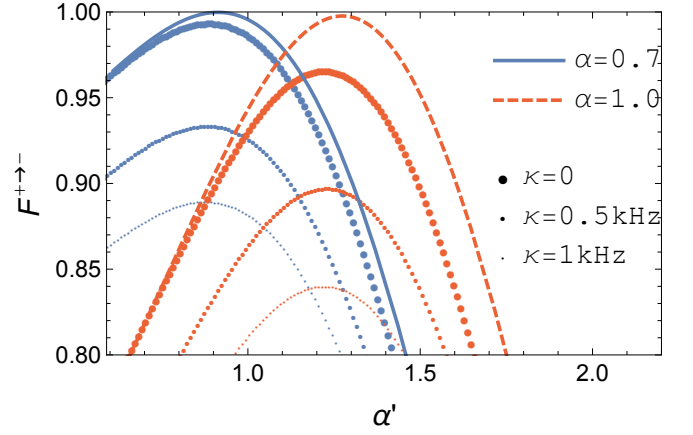


FIG. 4. Fidelity (Left) \mathcal{F}^{+-} with \hat{E}^\dagger from $|SC_\alpha^+\rangle$ to $|SC_\alpha^-\rangle$ ($\alpha' = G\alpha$). For ideal \hat{E}^\dagger on $|SC_\alpha^+\rangle$, the maximum fidelity values \mathcal{F}_{max}^{+-} are higher than 0.997 for $\{\alpha, \alpha'\} = \{0.7, 0.91\}, \{0.9, 1.23\}$ (in dashed, solid black) while dot lines (below the analytic curves) show the sensitivity of the performance against the different values of decoherence ($\gamma_- = \gamma^\phi = 10\kappa = 0, 5, 10\text{kHz}$) in simulation given by three sets of state-transfer operations.

abatically sweep the qubit frequency ω_q into resonance with the cavity, slowly transferring system into a superposition of dressed states $\sum_{n=0}^\infty c_n |+, n\rangle_{qc}$, where the c_n vanish for odd (even) n for even (odd) cat states. (3) A set of STIRAP-type pulses are performed in the manifolds of dressed states $\{|+, n\rangle, |-, n\rangle, |-, n+1\rangle\}$, in order, from the n -th to 0-th manifold. This produces a final state $\sum_{n=0}^\infty c_n |-, n\rangle$. (4) Finally, we blue detune the qubit frequency away from ω_r , thereby disentangling the qubit from the cavity and the final cavity state becomes $\sum_{n=0}^\infty c_n |n+1\rangle_c$ with the qubit in the ground state. In contrast to the original cavity QED proposals [28], π pulses can reset the qubit states $|g\rangle_q \rightarrow |e\rangle_q$ directly without affecting the cavity state [19], and hence $(\hat{E}^\dagger)^k$ can be performed by repeating the protocol.

For simulation, we examine a simplified driven JC Hamiltonian with two atomic levels [36, 37]

$$\begin{aligned} \hat{H}^{tot} = & \omega_r \left(\hat{a}^\dagger \hat{a} + \frac{1}{2} \right) + \frac{\omega_q}{2} \hat{\sigma}^z + \lambda (\hat{a}^\dagger \hat{\sigma}^- + \hat{a} \hat{\sigma}^+) \\ & + \sum_n \sum_{j=1}^2 \epsilon_j^n(t) \left(e^{-i\omega_j^n t} \hat{a} + e^{i\omega_j^n t} \hat{a}^\dagger \right), \end{aligned} \quad (9)$$

where ω_j^n are the frequencies the microwaves driving the cavity, and ϵ_j^n their strengths and Pauli operators are $\hat{\sigma}^z$ and $\hat{\sigma}^\pm$. We briefly note that this procedure in the driven JC system has a slightly different character to conventional STIRAP on a bared Λ -level atom with directly driven transitions (see Fig. 6 in the Supplementary Material). While the microwave driving terms in Eq. (9) couple all of the excitation subspaces of the undriven JC Hamiltonian, the Hamiltonian is only slightly perturbed

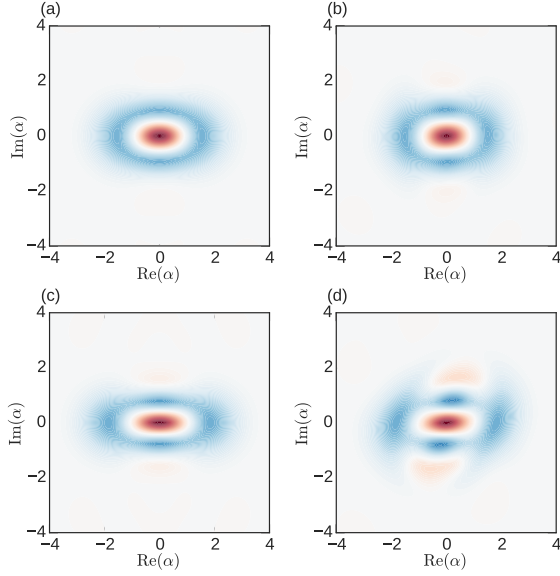


FIG. 5. Wigner functions for analytic $|SC_{\alpha'}^-\rangle$ and its numerical counterpart $\hat{E}^\dagger|SC_\alpha^+\rangle$ for (a) $\alpha' = 0.91$, (b) $\alpha = 0.7$, (c) $\alpha' = 1.23$ and (d) $\alpha = 1.0$. The fidelity is greater than 0.993 between (a) and (b) and above 0.965 between (c) and (d).

for small $|\epsilon_j|$ and pulse frequencies are far off-resonance from unwanted transitions. Thus, it leads to the majority of the evolution being confined to the respective $\{|\pm, n\rangle\}$ manifold. The bichromatic driving induces the transition $|+, n\rangle \rightarrow |-, n\rangle$ via quasi-adiabatic following even though the system is not (or close to) an eigenstate of the instantaneous Hamiltonian for part of the pulse sequence. This exploits the topological properties of the dressed eigenenergy surfaces [38].

Simulation with imperfections – To examine the performance of the protocol, we have numerically simulated the Hamiltonian Eq. (9) with cavity and qubit decay. Let us consider a single application of the ideal \hat{E}^\dagger acting on $|SC_\alpha^+\rangle$ analytically. The fidelity between $|SC_{\alpha'}^-\rangle$ and $\hat{E}^\dagger|SC_\alpha^+\rangle$ is given by

$$\mathcal{F}^{+\rightarrow-} = \left| \langle SC_{\alpha'}^- | \hat{E}^\dagger | SC_\alpha^+ \rangle \right|^2. \quad (10)$$

Fig. 4 shows that the maximum fidelity of $\mathcal{F}^{+\rightarrow-}$ of the ideal operation is higher than 0.997 with $\alpha = 0.7, 1.0$.

We examine three sets of STIRAP-type pulses to induce the transfer of $|+, n\rangle \rightarrow |-, n\rangle$ with $n = 0, 2, 4$ for the cases $\alpha = 0.7, 1.0$. The three sets cover enough of population of SCSs to achieve good amplification (see Fig. 7 in the Supplementary note). To model Markovian decoherence associated with cavity and qubit decoherence, we use a Lindblad master equation,

$$\dot{\rho} = i \left[\hat{H}^{tot}, \rho \right] + \kappa \mathcal{D}[\hat{a}] + \gamma_- \mathcal{D}[\hat{\sigma}^-] + \frac{\gamma_\phi}{2} \mathcal{D}[\hat{\sigma}^z], \quad (11)$$

where $\mathcal{D}[\hat{b}] = \hat{b}\rho\hat{b}^\dagger - \frac{1}{2}\{\hat{b}^\dagger\hat{b}, \rho\}$. To minimise the length

of the procedure and hence to reduce decoherence to practical levels, we perform all the transfers simultaneously and find that this produces almost same fidelities as three independent state-transfer sets. We use a single ω_1 which is shared between all transfers, adjusting Δ_i for each Λ -level system to find the appropriate value of ω_2^i . Our simulation parameters are $\lambda = 0.1$ GHz, $\omega_r = 6.0$ GHz, $\tau = 0.57\mu s$, $T = 1\mu s$, $|\epsilon_1| = 10$ MHz, $|\epsilon_2^0| = 35$ MHz, $|\epsilon_2^2| = 38$ MHz, $|\epsilon_2^4| = 50$ MHz, $\omega_1 = 5.949$ GHz, $\omega_2^0 = 5.749$ GHz, $\omega_2^2 = 5.603$ GHz, $\omega_2^4 = 5.501$ GHz, $\Delta_0 = 10$ MHz, $\Delta_2 = 14$ MHz, $\Delta_4 = 32$ MHz. With these parameters, the total state-transfer time is approximately $6\mu s$.

As shown in Figs. 4 and 5, the full simulation of the three sets without decoherence ($\gamma_- = \gamma^\phi = \kappa = 0$) is performed with maximum fidelity above 0.96 for both $\alpha = 0.7, 1.0$. This clearly shows the shift operation \hat{E}^\dagger has been performed on $|SC_\alpha^+\rangle$ and the components of the density matrix of SCSs are shifted by one Fock-basis element (see Fig. 8 in the Supplementary Material for details). Even without decoherence, a gap exists between the analytical and ideal cases, caused by the imperfections in the transfer method, and partly due to a small population of higher dressed states over $|+, 6\rangle$, which are not transferred. In Fig. 5, we present the Wigner functions of the final cavity state compared to an analytic SCS for $\alpha = 0.7, 1.0$ and a fringe pattern clearly appears with negative values. We see that the smaller SCS is amplified almost perfectly, while for $\alpha = 1.0$, phase shifts between the different number states causes distortion of the fringes in the Wigner functions. To model decoherence, we use $\gamma_- = \gamma^\phi = 10\kappa = 5, 10$ kHz using realistic parameters from Ref. [39] and the dotted points in Fig. 4 show that decoherence almost linearly reduces $\mathcal{F}^{+\rightarrow-}$ to 0.84 for our worst case ($\alpha = 1.0$ and $\kappa = 1$ kHz).

Summary and remarks – We have demonstrated a scheme for deterministic amplification of microwave SCSs using $(\hat{E}^\dagger)^2$ in circuit-QED. Based on a STIRAP-inspired state-transfer method, this amplification can be performed with a high fidelity under realistic decoherence. The deterministic and noiseless method overcomes the barrier to probabilistic amplification tools in optics-only methods by utilising artificial atomic states. In CV quantum information processing using SCSs, \hat{E}^\dagger can be used as a bit-flip operation, by switching the state parity with minimal amplification for $\alpha > 2$, while $(\hat{E}^\dagger)^2$ can act as a stabilizer operation on SCSs. If one can perform either \hat{E}^\dagger or $(\hat{E}^\dagger)^2$ depending on the outcome of a parity measurement of the cavity state, it can be used for a discretized purification of SCSs. Taking an advantage of well-separated lower energy levels, fluxonium or flux qubits can be also used for \hat{E}^\dagger [40]. The full analysis of driven JC system in the dressed-state representation for state-transfers will be investigated in the future [41].

Acknowledgements – We would like to thank J. Duningham for early contributions to this project and

H. Jeong and B. Vlastakis for useful comments. EG acknowledges support from EPSRC (EP/L026082/1). DKLO acknowledges the Quantum Information Scotland (QUISCO) network.

-
- [1] E. Schrödinger, *Naturwissenschaften* **23**, 823 (1935).
 - [2] H. M. Chrzanowski, N. Walk, S. M. Assad, J. Janousek, S. Hosseini, T. C. Ralph, T. Symul, P. K. Lam, *Nature Photon.* **8**, 333 (2014); J. B. Brask, I. Rigas, E. S. Polzik, U. L. Andersen, and A. S. Sørensen, *Phys. Rev. Lett.* **105**, 160501 (2010).
 - [3] H. Jeong and M. S. Kim, *Phys. Rev. A* **65**, 042305 (2002).
 - [4] C. R. Myers and T. C. Ralph, *New J. Phys.* **13**, 115015 (2011); T. C. Ralph, A. Gilchrist, G. J. Milburn, W. J. Munro, and S. Glancy, *Phys. Rev. A* **68**, 042319 (2003).
 - [5] A. P. Lund, T. C. Ralph, and H. L. Haselgrove, *Phys. Rev. Lett.* **100**, 030503 (2008).
 - [6] J. S. Neergaard-Nielsen, Y. Eto, C.-W. Lee, H. Jeong, and M. Sasaki, *Nature Photon.* **7**, 439 (2013).
 - [7] B. C. Sanders, *J. Phys. A* **45**, 244002 (2012); B. C. Sanders, *Phys. Rev. A* **45**, 6811 (1992) and references therein.
 - [8] J. Joo, W. J. Munro, and T. P. Spiller, *Phys. Rev. Lett.* **107**, 083601 (2011).
 - [9] A. A. Clerk, M. H. Devoret, S. M. Girvin, F. Marquardt, R. J. Schoelkopf, *Rev. Mod. Phys.* **82**, 1155 (2010); F. Ferreyrol, M. Barbieri, R. Blandino, S. Fossier, R. Tualle-Brouri, and P. Grangier, *Phys. Rev. Lett.* **104**, 123603 (2010); F. Ferreyrol, R. Blandino, M. Barbieri, R. Tualle-Brouri, and P. Grangier, *Phys. Rev. A* **83**, 063801 (2011); S. Pandey, Z. Jiang, J. Combes, and C. M. Caves, *Phys. Rev. A* **88**, 033852 (2013); J. Jeffers, *Phys. Rev. A* **83**, 053818 (2011); J. Jeffers, *Phys. Rev. A* **82**, 063828 (2010); E. Eleftheriadou, S. M. Barnett, and J. Jeffers, *Phys. Rev. Lett.* **111**, 213601 (2013); J. J. Fiurásek, *Phys. Rev. A* **80**, 053822 (2009); D. T. Pegg, L. S. Phillips, and S. M. Barnett, *Phys. Rev. Lett.* **81**, 1604 (1998).
 - [10] V. Parigi, A. Zavatta, M. Kim, and M. Bellini, *Science* **317**, 1890 (2007) and references therein.
 - [11] A. Zavatta, J. Fiurásek, and M. Bellini, *Nature Photon.* **8**, 564 (2014); N. A. McMahon, A. P. Lund, and T. C. Ralph, *Phys. Rev. A* **89**, 023846 (2014); G. Y. Xiang, T. C. Ralph, A. P. Lund, N. Walk, and G. J. Pryde, *Nature Photon.*, **4** 316 (2010); R. J. Donaldson, R. J. Collins, E. Eleftheriadou, S. M. Barnett, J. Jeffers, and G. S. Buller, *arXiv:1404.4277*.
 - [12] H. Jeong, A. Zavatta, M. Kang, S.-W. Lee, L. S. Costanzo, S. Grandi, T. C. Ralph, and M. Bellini, *Nature Photon.* **8**, 564 (2014).
 - [13] J. Park, J. Joo, and H. Jeong, in preparation.
 - [14] Z. Leghtas, S. Touzard, I. M. Pop, A. Kou, B. Vlastakis, A. Petrenko, K. M. Sliwa, A. Narla, S. Shankar, M. J. Hatridge, M. Reagor, L. Frunzio, R. J. Schoelkopf, M. Mirrahimi, and M. H. Devoret, *arXiv:1412.4633*.
 - [15] M. J. Everitt, T. P. Spiller, G. J. Milburn, R. D. Wilson, and A. M. Zagoskin, *arXiv:1212.4795*; L. Gilles and P. L. Knight, *Phys. Rev. A* **48**, 1582 (1993).
 - [16] H. Jeong, A. P. Lund, and T. C. Ralph, *Phys. Rev. A* **72**, 013801 (2005); A. P. Lund, H. Jeong, T. C. Ralph, and M. S. Kim, *Phys. Rev. A* **70**, 020101(R) (2004); J. Etesse, M. Bouillard, B. Kanseri, and R. Tualle-Brouri, *arXiv:1412.3219*.
 - [17] A. Laghaout, J. S. Neergaard-Nielsen, I. Rigas, C. Kragh, A. Tipsmark, and U. L. Andersen, *Phys. Rev. A* **87**, 043826 (2013).
 - [18] A. Ourjoumtsev, R. Tualle-Brouri, J. Laurat, P. Grangier, *Science* **312**, 83 (2006); A. Ourjoumtsev, H. Jeong, R. Tualle-Brouri, and P. Grangier, *Nature* **448**, 784 (2007); J. S. Neergaard-Nielsen, B. Melholt Nielsen, C. Hettich, K. Mølmer, and E. S. Polzik, *Phys. Rev. Lett.* **97**, 083604 (2006) and references therein.
 - [19] B. Vlastakis, G. Kirchmair, Z. Leghtas, S. E. Nigg, L. Frunzio, S. M. Girvin, M. Mirrahimi, M. H. Devoret, and R. J. Schoelkopf, *Science* **342**, 607 (2013).
 - [20] M. Hofheinz, H. Wang, M. Ansmann, R. C. Bialczak, E. Lucero, M. Neeley, A. D. O'Connell, D. Sank, J. Wenner, J. M. Martinis, and A. N. Cleland, *Nature* **459**, 546 (2009).
 - [21] A complementary version of amplifying SCSs (continuous-amplification) could be performed in specially engineered circuit-QED [14].
 - [22] Z. Leghtas, G. Kirchmair, B. Vlastakis, R. J. Schoelkopf, M. H. Devoret, and M. Mirrahimi, *Phys. Rev. Lett.* **111**, 120501 (2013).
 - [23] M. Mirrahimi, Z. Leghtas, V. V. Albert, S. Touzard, R. J. Schoelkopf, L. Jiang, and M. H. Devoret, *New J. Phys.* **16**, 045014 (2014).
 - [24] C. C. Gerry and P. L. Knight, *Introductory Quantum Optics* (Cambridge University Press, Cambridge, U.K., 2005).
 - [25] L. S. Bishop, J. M. Chow, J. Koch, A. A. Houck, M. H. Devoret, E. Thuneberg, S. M. Girvin, R. J. Schoelkopf, *Nature Physics* **5**, 105 (2009); L. S. Bishop, Ph.D. thesis, Yale University (2010), *arXiv:1007.3520*.
 - [26] B. R. Johnson, Ph.D. thesis, Yale University (2011).
 - [27] A. Kuhn, M. Hennrich, T. Bondo, and G. Rempe, *Appl. Phys. B: Lasers and Optics* **69**, 373–377 (1999).
 - [28] A. S. Parkins, P. Marte, P. Zoller, and H. J. Kimble, *Phys. Rev. Lett.* **71**, 3095 (1993); A. S. Parkins, P. Marte, P. Zoller, O. Carnal, and H. J. Kimble, *Phys. Rev. A* **51**, 1578 (1995).
 - [29] X. Zou, J. Shu, and G. Guo, *Phys. Lett. A* **359**, 117 (2006).
 - [30] D. K. L. Oi, J. Jeffers, and V. Potoček, *Phys. Rev. Lett.* **110**, 210504 (2013).
 - [31] \hat{E}^\dagger is an isomorphism but is not unitary since $\hat{E}^\dagger \hat{E} \neq \mathbb{I}$.
 - [32] G. Falci, A. La Cognata, M. Berritta, A. D'Arrigo, E. Paladino, and B. Spagnolo, *Phys. Rev. B* **87**, 214515 (2013).
 - [33] N. A. Masluk, Ph.D. thesis, Yale University (2012).
 - [34] B. R. Johnson, M. D. Reed, A. A. Houck, D. I. Schuster, L. S. Bishop, E. Ginossar, J. M. Gambetta, L. DiCarlo, L. Frunzio, S. M. Girvin, and R. J. Schoelkopf, *Nature Phys.* **6**, 663 (2010).
 - [35] E. Ginossar, L. S. Bishop, D. I. Schuster, and S. M. Girvin, *Phys. Rev. A* **82**, 022335 (2010).
 - [36] P. Alsing, D. S. Guo and H. J. Carmichael, *Phys. Rev. A* **45**, 5135 (1992).
 - [37] A. Blais, R. S. Huang, A. Wallraff, S. M. Girvin, and R. J. Schoelkopf, *Phys. Rev. A* **69**, 062320 (2004).
 - [38] M. Amnat-Talab, S. Lagrange, S. Guérin and H. R. Jauslin, *Phys. Rev. A* **70**, 013807 (2004).
 - [39] M. H. Devoret and R. J. Schoelkopf, *Science* **339**, 1169

- (2013).
- [40] V. E. Manucharyan, J. Koch, L. I. Glazman, and M. H. Devoret, *Science* **326**, 113 (2009); G. Zhu and J. Koch, *Phys. Rev. B* **87**, 144518 (2013).
- [41] J. Joo, M. Elliott, D. K. L. Oi, E. Ginossar, and T. Spiller, in preparation.

SUPPLEMENTARY NOTE

Evidence of STIRAP-type operations

Although this STIRAP-type operation behaves well enough for our desired state-transfer ($|+, n\rangle \rightarrow |-, n\rangle$), the details of the proposed state-transfer cannot be explained by conventional STIRAP in a bare Λ atomic system. In STIRAP, the overlap of the two pulse envelopes is a crucial parameter to determine the state-transfer efficiency [1]. In particular, efficient state-transfer only occurs for the counter-intuitive sequence of the two pulses (ϵ_1^0 first and ϵ_2^0 second).

We have examined the transfer efficiency of our scheme for the simplest transfer from $|+, 0\rangle$ to $|-, 0\rangle$ with detuning Δ_0 in Fig. 6. For positive τ , the behaviour is similar to the normal STIRAP counter-intuitive pulse sequence, with transfer efficiency rapidly increasing as τ increases, nearly reaching 1 plateauing. The efficiency then drops with decreasing overlap area. However, the suggested STIRAP-type operation also shows excellent state-transfer for the reverse pulse sequence.

In our parameter region, and without decoherence, the transfer efficiency is symmetric about $\tau = 0$ (fully overlapped pulses). However, the transfer efficiency for reversed pulses is more sensitive to changes in Δ_0 and the length of pulse envelopes. Oscillations are seen in the transfer efficiency, indicating that the process may not be ‘as adiabatic’ as conventional STIRAP. These phenomena might be better understood in adiabatic Floquet theory [2] and we believe they are caused by the existence of energy levels outside the Λ -system [3]. Further detailed

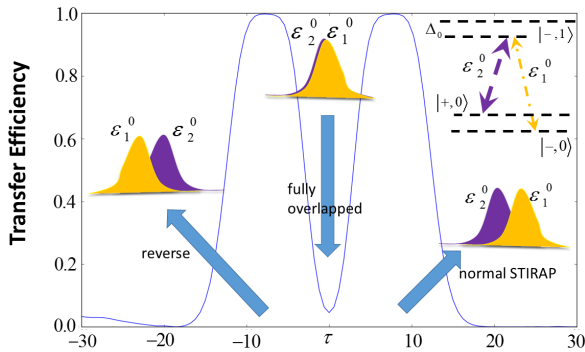


FIG. 6. Transfer efficiency of the STIRAP-like pulses as a function of the overlap between the two pulses.

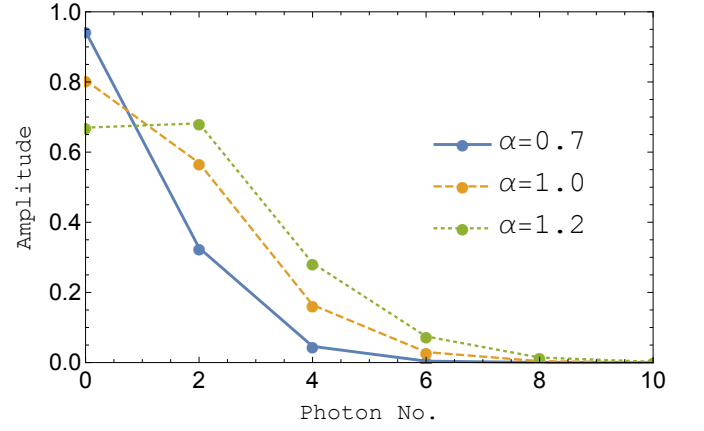


FIG. 7. Photon number amplitudes for $|SC_\alpha^+\rangle$ for $\alpha = 0.7, 1.0, 1.2$.

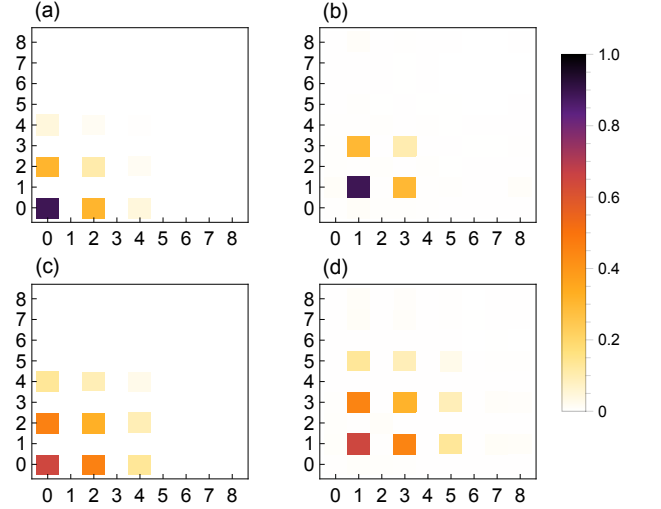


FIG. 8. Simulated density matrix plots for (a) $|SC_{0.7}^+\rangle$, (b) $\hat{E}^+|SC_{0.7}^+\rangle$, (c) $|SC_{1.0}^+\rangle$, and (d) $\hat{E}^+|SC_{1.0}^+\rangle$ without decoherence. They indicate that the shift operation \hat{E}^+ is performed with high fidelity on $|SC_\alpha^+\rangle$.

investigation of the driven JC system in the dressed-state representation for this STIRAP-type operation will be presented in later work [4].

Amplitude distribution for even SCSs

In order to perform \hat{E}^+ efficiently and practically, the minimum number of STIRAP-type sets can be decided by the plot of amplitudes of SCSs. Fig. 7 shows that $|SC_{0.7}^+\rangle$ and $|SC_{1.0}^+\rangle$ have most of their populations in three Fock states, $\{|0\rangle, |2\rangle, |4\rangle\}$, with the population in $|6\rangle$ starting to contribute significantly for $|SC_{1.2}^+\rangle$. Thus, four or more sets of STIRAP-type operations are required for even SCSs at $\alpha > 1.2$ to obtain a high fidelity \hat{E}^+ .

Evidence of \hat{E}^\dagger operation on $|SC_\alpha^+\rangle$

It is relatively straightforward to show the performance of \hat{E}^\dagger with a density matrix of the final state. For example, we can write the density matrix of the initial even SCS

$$\rho_{int} = |SC_\alpha^+\rangle\langle SC_\alpha^+| = \sum_{n,m=0}^{\infty} c_{nm} |2n\rangle\langle 2m|. \quad (12)$$

Then, if the one-photon shift operation has been performed,

$$\rho_{out} = \hat{E}^\dagger |SC_\alpha^+\rangle\langle SC_\alpha^+| \hat{E} = \sum_{n,m=0}^{\infty} c_{nm} |2n+1\rangle\langle 2m+1|, \quad (13)$$

As shown in Fig. 8, the coefficient c_{nm} have been preserved while the Fock basis has been shifted for $|SC_{0.7}^+\rangle$ and $|SC_{1.0}^+\rangle$. This type of quantum process tomography has already been performed experimentally and SCSs in a high-Q cavity field can be measured through a low-Q cavity via a superconducting qubit [5]. One can assume that the initial SCS is prepared using the method of Ref. [5], and that the \hat{E}^\dagger operation can be performed twice with the assistance of the sandwiched superconducting qubit. As explained in the protocol, the outcome state is ideally expected to be $|g\rangle_q |SC_{\alpha'}^+\rangle_c$ with high fidelity. Using Ramsey interferometry, one can measure the qubit state-dependent phase shift of the cavity state, with de-

tailed methods explained in the Supplementary Materials of Ref. [5], then one can perform tomography on the state in the high-Q cavity through the low-Q cavity. Alternatively, a parity measurement experiment can also be used to show the parity difference between initial state $|SC_\alpha^+\rangle$ and $\hat{E}^\dagger |SC_\alpha^+\rangle$ [6].

References

- [1] P. Král, I. Thanopoulos, and M. Shapiro, Rev. Mod. Phys. **79** 53, (2007); D. Møller, J. L. Sørensen, J. B. Thomsen, M. Drewsen, Phys. Rev. A **76**, 062321 (2007).
- [2] K. Dresea and M. Holthausb, Eur. Phys. J. D **5**, 119 (1999); R. Unanyan, S. Guérin, B.W. Shore, and K. Bergmann, Eur. Phys. J. D **8**, 443 (2000).
- [3] V. S. Malinovsky and D. J. Tannor, Phys. Rev. A **56**, 4929 (1997); N.V. Vitanov, B.W. Shore, and K. Bergmann, Eur. Phys. J. D **4**, 15 (1998).
- [4] J. Joo, M. Elliott, D. K. L. Oi, E. Ginossar, and T. Spiller, in preparation.
- [5] B. Vlastakis, G. Kirchmair, Z. Leghtas, S. E. Nigg, L. Frunzio, S. M. Girvin, M. Mirrahimi, M. H. Devoret, and R. J. Schoelkopf, Science **342**, 607 (2013).
- [6] L. Sun, A. Petrenko, Z. Leghtas, B. Vlastakis, G. Kirchmair, K. M. Sliwa, A. Narla, M. Hatridge, S. Shankar, J. Blumoff, L. Frunzio, M. Mirrahimi, M. H. Devoret, and R. J. Schoelkopf, Nature **511**, 444 (2014).